

Supporting Green Neuromorphic Computing: Machine Learning Guided Microfabrication for Resistive Random Access Memory

Abdi Yamil Vicencio del Moral, Md Mehedi Hasan Tanim, Feng Zhao, Xinghui Zhao
School of Engineering and Computer Science
Washington State University Vancouver
Vancouver, WA

Email: {a.vicencio del moral, mehedi.tanim, feng.zhao, x.zhao}@wsu.edu

Abstract—The growing popularity of big data and machine learning applications call for a more powerful and energy-efficient way to execute deep learning workflows. Neuromorphic chips provide a potential solution, as they attempt to mimic the neuronal architectures in human brain and show great potentials in reducing energy consumption in the order of magnitude and also improve the computational performance. However, the fabrication process for neuromorphic chips is costly and currently based on trial-and-error, which adds complexity to the design process. In this paper, we address these challenges by designing and developing machine learning guided microfabrication process for Resistive Random Access Memory (RRAM), which is a key device in neuromorphic chips. Specifically, our research makes the following contributions: 1) we successfully fabricated a new RRAM using bio-organic materials, leading to a greener solution for supporting neuromorphic computing; 2) we carried out a comprehensive study on the microfabrication process conditions and their effects on the RRAM devices, producing new knowledge to the field; 3) we developed a synthetic data assisted approach to predict key performance metrics of the bio-organic RRAM (bio-RRAM) devices, without requiring substantial amount of experimental training data; and 4) we developed a more advanced approach which leverages learning task conversion to make predictions on fine-grained performance metrics with no added requirements for experimental or synthetic data. We evaluated these approaches using eight honey-based bio-RRAM devices we fabricated, and the results show that both approaches are effective in terms of predicting the devices performance. We expect that the machine learning guided microfabrication will pave the way to more efficient and effective design of the next-generation RRAM devices for green neuromorphic computing.

Index Terms—Resistive Random Access Memory; Neuromorphic Computing; Machine Learning; Big Data; Microfabrication

I. INTRODUCTION

Current computing technology is relying on von Neumann architecture hardware [1], which requires significant amount of power to run repeated transient operations with vast amount of data exchanged [2]. In order to address the challenge of enhancing computing capability with much lower power consumption, neuromorphic computing, a computing system with hardware emulating biological structure and functions of a human brain, was identified as the promising solution [3], [4]. Neuromorphic chips implement artificial neurons and synapses hardware to execute bio-inspired machine learning

algorithms in a more energy-efficient way. Artificial synaptic devices based on non-volatile resistive switching random access memory (RRAM) are considered as the most adoptable technology due to the simplified device architecture and low-cost manufacturing process, ability to store huge amount of data in limited space, and capability of emulating functions of a synapse. The two terminal metal-insulator-metal (MIM) structure of these devices resembles biological neural synapse, as shown in Figure 1.

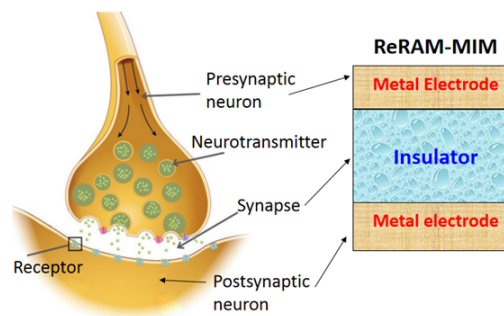


Fig. 1. Resemblance of RRAM MIM structure to biological neural synapse.

Despite their great potentials, for the development of RRAM based neuromorphic systems, substantial gaps still exist at the hardware and software layers, as well as the interface between them. Specifically, insulator materials such as inorganic metal oxides [5]–[9], polymers [10], and natural bio-organic materials [11]–[14] derived from living or once-living organisms, mainly protein and carbohydrate, are being investigated as the active switching layer. Among these materials, natural bio-organic materials are renewable, sustainable, environmentally friendly, biocompatible, biodegradable and abundant in nature, therefore desirable for “green” electronic and neuromorphic systems. However, some critical issues must be addressed for bio-organic materials based RRAM, i.e. bio-RRAM, such as understanding of the conduction mechanism governing memory and synaptic properties, evaluation of the impacts of film processing conditions on device performance, and utilize machine learning and data analytics techniques to guide

microfabrication processes. In this paper, we address these challenges by developing an effective approach to model and predict the performance of RRAM devices, which can be used to guide the microfabrication process for supporting more efficient and effective neuromorphic hardware design.

Our approach presented in this paper bridges the gaps in the state-of-the-art research by making the following contributions. First, we successfully developed RRAMs using natural bio-organic materials as the active switching layer, and demonstrated their effectiveness as synaptic devices. Second, we carried out a comprehensive analysis on the correlation of biomaterial film process, film property and bio-RRAM device performance, providing a foundation for better understanding of the effects of fabrication process conditions on the device performance. Third, we developed machine learning algorithms to learn from the process-performance correlation and predict optimal film process conditions and device synaptic properties. Finally, we addressed the fundamental challenge of training data availability, and significantly reduced the requirement for training data in performing the learning tasks. We have evaluated our approach using real experimental data collected during the microfabrication processes, and our results demonstrated the effectiveness of this approach and its great potentials in guiding more efficient microfabrication for novel RRAM devices.

The rest of the paper is organized as follows. Section II reviews the state-of-the-art research in RRAM based neuromorphic computing, as well as data analytics for its microfabrication processes. In Section III, we present our work in developing bio-RRAM and the dataset obtained during the fabrication process. Section IV presents an approach for synthetic data assisted prediction for bio-RRAM performance. In Section V, we present a different approach in which machine learning is used to predict the performance distribution, leading to a full understanding of the bio-RRAM devices without significant fabrication cost. Both approaches were evaluated using eight honey-based bio-RRAM devices we fabricated. Finally, we conclude the paper in Section VI.

II. RELATED WORK

Recent advances in big data computing and machine learning present unprecedented challenges for the traditional von Neumann architecture hardware technology, which consumes a significant amount of energy to execute repeated transient operations with increasing data exchange. In order to enhance computing capability with much lower power consumption, “brain-like” neuromorphic computing was identified as the promising solution. Such analog systems require hardware components capable of mimicking human synapse [15]–[17], the basic building block of biological neural network. Artificial synaptic devices based on nonvolatile memory technologies such as ferroelectric random access memory (RAM), magnetic RAM, phase-change RAM, and resistive RAM (RRAM) [18] have been investigated. Of these technologies, RRAM is adoptable due to its merits of simple and scalable device architecture, low power operation, high switching speed, good

retention and endurance, CMOS and 3D integration, and low manufacturing cost.

In recent years, bio-RRAM with the active resistive switching layer made from natural organic materials such as gelatin, albumen, cellulose, chitosan, lignin, pectin, aloe polysaccharide, fructose, glucose, honey, etc. have been reported [19]–[26]. With continuous development and progress in design and microfabrication process, some of these devices are achieving reasonable memory characteristics that are required by non-volatile memory, including set and reset voltages, read voltage window, on/off ratio, endurance cycles, and retention time.

The microfabrication process for RRAMs involves many parameters which may significantly affect film properties, resulting in varying synaptic functions of the fabricated RRAM devices. For instance, the drying conditions during the fabrication process, e.g., temperature, duration, etc., can affect the density of electron trap centers which commonly originate from imperfection of molecular chains of compounds during the process of transformation from raw precursor to solidified thin film. Also, the more hydroxy groups, the deeper the traps are formed in the interstitial space when cross-linked and branched network occur due to the high solidifying temperature. In addition, the materials used in the electrodes also affect the device performance, as the low resistance state (LRS) of RRAM depends strongly on the resistance of electrodes. Traditionally, the selection of these process parameters are based on “trial and error”, without a comprehensive understanding of the quantified correlations between the parameters and their effects on the product devices.

Most recently, with the growing interest in applying machine learning techniques to various experimental based research, some research has been done in developing machine learning based methods for assisting microfabrication processes. For example, artificial neural networks have been used to study the effects of processing parameters on the geometry of femtosecond laser fabricated microgrooves on 4H-SiC wafer [27]. Support vector machines have been used to optimize parameters for laser-magnetic welding [28]. A random forest ensemble based method is developed to predict stent dimensions in microfabrication processes [29]. To the best of our knowledge, there is no prior work on modeling microfabrication processes and predicting the synaptic performance of RRAM devices. The research presented in this paper provides such an approach to bridge the gap.

III. BIO-RRAM SAMPLES AND DATASET

A. Microfabrication Process for Bio-RRAM

In this study, eight bio-RRAM samples with the honey film as the resistive switching layer were fabricated under different conditions as shown in Table I.

The fabrication started with eight 2.5 cm × 2.5 cm glass slides (sample ID numbered by 1-8) used as the substrate and cleaned thoroughly by acetone, isopropyl alcohol and de-ionized water in an ultrasonic bath. After cleaning, four glass slides were covered by indium tin oxide (ITO) and the other four by copper (Cu) as the bottom electrode. Two bottles of

TABLE I
SUMMARY OF BIO-RRAM SAMPLES

Sample ID	Bottom Electrode	Resistive Switching Film	Baking Temp (°C)	Baking Time (hrs)
1	ITO	Pure Honey	140	2
2	ITO	Pure Honey	140	4
3	ITO	Pure Honey	90	8
4	Cu	Pure Honey	140	2
5	Cu	Pure Honey	90	8
6	ITO	Honey/CNT	90	8
7	Cu	Honey/CNT	140	2
8	Cu	Honey/CNT	90	8

honey solutions were prepared by mixing pure raw honey with de-ionized (DI) water at room temperature until no honey crystal was visible. The honey concentration was 30% by weight in the final honey solution. No stirring was applied to avoid air bubbles in the honey solution. Next, single wall carbon nanotube (CNT) powders was dispersed in one honey solution in an ultrasonic bath for 60 mins to form honey/CNT solution with a 0.2 wt% concentration of CNT. The honey thin film with or without CNT was formed by spin-coating pure honey solution or honey/CNT solution on the sample at 1000 rpm for 90 s, followed by baking on a hotplate at two different temperatures of 90°C and 140°C for three different durations of 2, 4 and 8 hours for comparison study. Finally, a shadow mask with circular patterns of 500 μm -diameter was used to cover the honey film and 100 nm-thick aluminum (Al) top electrodes were deposited on the dried honey film to complete the honey-RRAM fabrication. Resistive switching characteristics of the honey-RRAM devices were performed with the sample on a probe-station by a semiconductor characterization system in air and at room temperature. During all electrical measurements, voltage bias was applied on the Al top electrode while the ITO or Cu bottom electrode remained grounded.

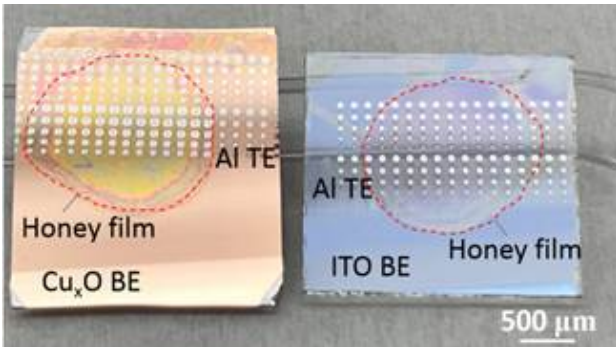


Fig. 2. Photographs of Honey-based Bio-RRAMs

Figure 2 shows two example bio-RRAM devices we fabricated through this process. The 8 bio-RRAM samples are used to generate the data required for this research.

B. Dataset

Through the microfabrication process described in Section III-A, we have obtained an initial dataset which will be

used in the subsequent analysis and learning tasks. Table I shows the summary of 8 honey-based bio-RRAM samples with their specific process conditions. In addition to the process conditions shown in Table I, we used 3 fixed conditions for all samples: 30% honey concentration (by weight), 3000 rpm spin-coating rate, and Aluminum as the top electrode material. These fixed parameters are chosen based on our past experience [26], aiming for simplifying the microfabrication process and allowing more focused study on the effects of other critical process conditions. We have carried out a preliminary study on these honey-based RRAM devices [30], and our results show that nonvolatile bipolar switching memory characteristics were observed when electrical testing was conducted on honey-based RRAM devices. These switching capabilities in RRAM devices are the essential attributes that provide the potential for mimicking synaptic plasticity.

To further study the characteristics of the 8 bio-RRAM samples, we have carried out extensive experiments to test their performance. Here in this paper we will use the SET voltage as a target property. Note that the approach presented in this paper can be easily applied to any performance metrics of bio-RRAM devices. We use SET voltage in this study because it is a key property for both memory and synaptic functions. SET voltage values were extracted during the experiment process in which a positive voltage sweep was applied to the RRAM device. During the positive sweep, the current was gradually increased until compliance was reached at the SET voltage, indicating the change from a high resistance state (HRS) to a low resistance state (LRS) of the honey film layer.

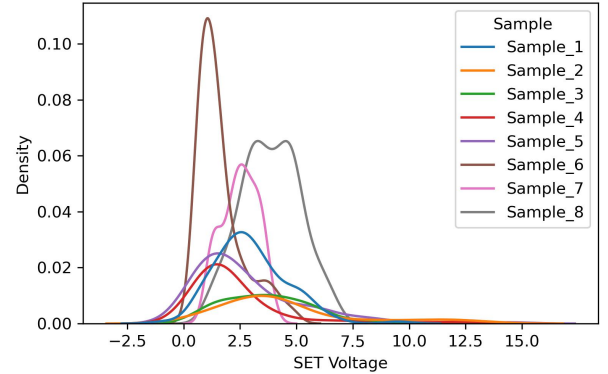


Fig. 3. SET Voltages of Honey-Based Bio-RRAM Samples

Figure 3 shows the probability density functions (PDF) of the measured SET voltages of these samples. Specifically, for each sample device i ($1 \leq i \leq 8$), the figure shows the probability density function for its SET voltage values $f_i(x)$, where

$$P[V_{SET1} < X < V_{SET2}] = \int_{V_{SET1}}^{V_{SET2}} f_i(x) dx$$

As shown in Figure 3, the switching performance of the 8 samples vary significantly, indicating that the film processing can greatly alter the properties of biomaterial as the resistive film and ultimately the bio-RRAM device performance. Therefore it is essential to correlate film process conditions, film properties and device synaptic characteristics. Currently optimization of biomaterial film process and bio-RRAM synaptic properties rely on conventional “trial and error” practice which requires large numbers of development cycles. Accurately predicting device synaptic properties by less process trial cycles will expedite the development of bio-RRAM for the realization of green neuromorphic systems.

When applying machine learning techniques to experimental fields such as semiconductor and material science, a fundamental challenge is the availability of training data. Due to the fact that collecting training data from the microfabrication process is extremely costly, machine learning algorithms have not been widely adopted in this process. We address this challenge using two different approaches: 1) developing synthetic data generation methods which can aid the machine learning prediction on the key statistical metrics; and 2) applying machine learning methods to predict the probabilities of certain measurements, which can be used to assist the microfabrication process by providing guidance on potential process conditions which will likely lead to desired device performance. These approaches are described in the following sections.

IV. SYNTHETIC DATA ASSISTED PREDICTION

A. Methodology

As the first step toward predicting the synaptic performance of bio-RRAM devices, we use a set of statistical metrics to represent bio-RRAM performance, and explore the potentials of machine learning models in predicting such metrics based on the input features, i.e., microfabrication process conditions. The statistical metrics chosen include mean, standard deviation, minimum and maximum values. Table II shows the statistical metrics for the 8 bio-RRAM samples. As shown in the table, the metrics for different samples vary, and the variance is introduced by the microfabrication process.

TABLE II
STATISTICAL METRICS OF SET VOLTAGES FOR BIO-RRAM SAMPLES

Sample ID	SET Mean	SET STD	SET Min	SET Max
1	2.977045	1.597761	-0.875	9.50
2	4.425900	2.986744	0.675	12.72
3	3.647100	1.849857	0.500	8.20
4	2.333061	2.334147	0.550	13.40
5	2.808100	2.466977	0.275	14.40
6	1.614227	1.017776	0.460	4.96
7	2.491638	0.783879	0.920	4.08
8	3.863131	1.296368	1.00	6.76

These statistical metrics capture the main characteristics of the device performance in terms of SET voltage values, therefore, predicting these metrics for new samples can provide critical guidance on process condition selection in the

microfabrication process. The ultimate goal of this approach is to develop machine learning based methods to learn the correlations between the process conditions and the statistical metrics of the target values. In this case, the target values are the SET voltages for the bio-RRAM devices.

As mentioned earlier, a fundamental challenge in utilizing machine learning techniques in the microfabrication field is the cost of obtaining experimental data. Given the fact that each sample requires a lengthy and demanding fabrication process, it is extremely difficult to collect a large amount of samples for training. With limited amount of training data, adopting machine learning approaches has been challenging. To address this challenge, we will leverage a two-phase machine learning approach, in which the first phase is designed for generating synthetic data, and the second phase will use the synthetic data for training, in addition to the experimental data.

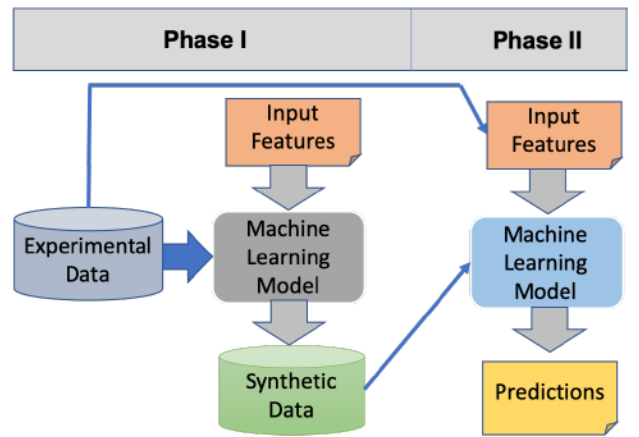


Fig. 4. Synthetic Data Assisted Prediction

Figure 4 depicts the 2-phase approach for predicting bio-RRAM performance. In Phase I, experimental data obtained from the bio-RRAM is used as *seed* to train a machine learning model. The trained model will then be used as a synthetic data generator, which takes input data features, i.e., microfabrication process conditions, and generate synthetic data, aiming for expanding data samples without the costly fabrication process. In Phase II, the synthetic data is combined with the experimental data to form a training dataset to train a machine learning model for making predictions based on any process conditions. This approach addresses the training data challenge leveraging the sequential machine learning data synthesis [31], which has been proven to be an effective approach for synthetic data generation.

This approach can be applied to each performance metric to generate sufficient data samples as needed. Algorithm 1 illustrate the workflow for generating synthetic datasets, which will be used for training the Phase II models for predicting the four statistical metrics.

B. Experimental Design

In order to establish a comprehensive understanding on the proposed approach, We have implemented the methodology

Algorithm 1: Sequential Machine Learning Data Synthesis

Input: Experimental Dataset

Output: Synthetic Datasets

Result: Sufficient synthetic data is generated for each target performance metric

Create dataset A using experimental data with process conditions as features and SET voltage mean as target;

while *More synthetic data is needed* **do**

 Build regression model $F1$ on A ;

 Synthesize data set B as $B1' = F1(B)$ where $B1'$ is the predicted SET Voltage mean value;

 Modify data set A to include the SET voltage standard deviation as the new target;

 Build regression model $F2$ on A ;

 Input B with as $B2' = F2(B)$ where $B2'$ is the predicted standard deviation value;

 Modify data set A to include the difference of the mean and minimum SET voltage as the new target;

 Build regression model $F3$ on A ;

 Input B with as $B3' = F3(B)$ where $B3'$ is the difference of the mean and minimum value;

 Modify data set A to include the difference of the mean and maximum SET voltage as the new target;

 Build regression model $F4$ on A ;

 Input B with as $B4' = F4(B)$ where $B4'$ is the difference of the mean and maximum value;

$A = A + B$;

end

described in Section IV-A using various machine learning regression models. The models used in our study are listed as follows, representing a comprehensive coverage in commonly used regression models.

- **Linear Regression:** Linear Regression is an algorithm that aims to fit a line to the data by estimating regression coefficients and minimizing the residual sum of squares between the observed targets and the predicted targets.
- **Random Forest Regression:** Random Forest Regression is a type of model that constructs a number of decision trees on subsamples of the dataset and combines the predictions to improve the overall predictive accuracy and prevent over-fitting.
- **Support Vector Machine:** Support vector machine is a type of algorithm whose main objective is to find a hyperplane in a feature space such that it can distinctly classify the data points.
- **Kernel Ridge Regression:** This algorithm combines ridge regression with the use of kernel functions that allows it to operate in a high-dimensional feature space.

- **AdaBoost Regression:** AdaBoost is an ensemble method that fits a regressor on a data set, then adjusts the weights of the instances based on the prediction error and commences to fit more copies of the regressor on the dataset.

These regression models are integrated in Algorithm 1 to perform synthetic data generation and performance prediction for each of the four statistical metric. Note that generating new data instances involved creating new combinations for the processing conditions of bottom electrode material, resistive switching film, baking temperature, and baking time. When generating synthetic data samples, the following guidelines are used. Temperature values were incremented by 10 degrees for each instance starting at 90 degrees Celsius up to 140 degree Celsius. Baking time duration values were decremented from 4 hours to 2 hours, incremented from 4 hours to 8 hours, and incremented from 8 hours to 10 hours by half hours steps. The dataset is a combination of all the features values including bottom electrode material, top electrode material, resistive switching film, baking temperature ($^{\circ}\text{C}$), and baking time (hours). A total of 176 new data instances for potential RRAM processing conditions were generated.

C. Evaluation

To evaluate the effectiveness of our 2-phase approach described in Section IV-A, we have carried out two sets of experiments as follows.

- **Experiment 1** (8 sample test): In this experiment, we use all eight bio-RRAM samples in Phase I for synthetic data generation. Once sufficient amount of synthetic data is generated, only the synthetic dataset is used in Phase II for training. Then the original 8 sample dataset is used for to evaluate the trained model in Phase II.
- **Experiment 2** (7 and 1 sample test): In this experiment, we use a leave-one-out approach to enable a more rigorous test. Specifically, we take Sample 4 out from the original bio-RRAM dataset, and use the rest 7 samples in Phase I for synthetic data generation. Once sufficient amount of synthetic data is generated, only the synthetic dataset is used in Phase II for training. Then we run two tests: 1) **7 sample test:** the 7 bio-RRAM samples are used to evaluate the trained model; and 2) **1 sample test:** Sample 4 is used for testing the trained model. This is the sample that has never been included in the previous steps. The goal is to use a real sample with a new set of input features to test the accuracy of the model prediction.

For evaluation, we use the typical metrics for evaluating the accuracy of regression models, Mean Square Error (MSE) and Root Mean Square Error (RMSE). These metrics indicate the average deviation between the predicted data points and the actual data points. The definitions of these metrics are listed as follows.

$$mse = \left(\frac{1}{n}\right) \sum_{i=1}^n (\hat{y}_i - y_i)^2$$

$$rmse = \sqrt{mse}$$

where $\hat{y}_i = predicted$ and $y_i = actual$

Experiments have been carried out to evaluate the 2-phase approach for predicting 4 target statistical metrics for bio-RRAM SET voltages: mean, standard deviation, minimum, and maximum. Using the mean metric as an example, we present the experimental results for the 2-phase approach. Table III shows the results obtained in Experiment 1 (8 sample test). Table IV shows the results obtained in Experiment 2 (7 sample test), and Table V shows the results of Experiment 2 (1 sample test), in which we predict the the SET voltage mean value for Sample 4, which is not included in the prior process of the experiments.

TABLE III
PREDICTION ACCURACY FOR SET VOLTAGE MEAN (EXPERIMENT 1: 8 SAMPLE TEST)

Machine Learning Model	MSE	RMSE
Linear Regression	0.53	0.73
Random Forest Regression	0.18	0.43
Support Vector Machine	0.73	0.85
Kernel Ridge Regression	0.56	0.75
AdaBoost Regression	0.06	0.24

TABLE IV
PREDICTION ACCURACY FOR SET VOLTAGE MEAN (EXPERIMENT 2 - 7 SAMPLE TEST)

Machine Learning Model	MSE	RMSE
Linear Regression	0.61	0.78
Random Forest Regression	0.21	0.46
Support Vector Machine	0.76	0.87
Kernel Ridge Regression	0.58	0.76
AdaBoost Regression	0.04	0.19

TABLE V
PREDICTION ACCURACY FOR SET VOLTAGE MEAN (EXPERIMENT 2: 1 SAMPLE TEST)

Machine Learning Model	Mean	MSE	RMSE
True Sample 4 Data	2.33306	–	–
Linear Regression	3.3986	1.14	1.07
Random Forest Regression	2.970	0.41	0.64
Support Vector Machine	3.091	0.58	0.76
Kernel Ridge Regression	3.103	0.59	0.77
AdaBoost Regression	2.8081	0.23	0.48

As shown in the results, all machine learning models perform reasonably well, with MSE values less than 0.9 for both 8 sample and 7 sample tests. Notably, AdaBoost outperform other models in predicting mean values of SET voltages. For the 1 sample test, where Sample 4 is used as the testing data, the machine learning models show similar performance as the previous tests, with MSE values ranging from 0.2 to 1.1. AdaBoost again outperforms others and achieved prediction error less than 0.5. These results show that the 2-phase synthetic data based approach is effective

in achieving accuracy prediction on statistical metrics without requiring a substantial number of training samples.

Even though the synthetic data can help address the training data challenges, there several disadvantages to using synthetic data that researchers should consider. One such disadvantage is that generated data may have biased information, especially in a small dataset [32]. It may also be unrealistic and a poor representation of real world data. For example, the models may provide predictions for temperature levels that would not be appropriate to use in the fabrication of RRAM devices. However with careful analysis, synthetic data can provide insight on correlations that may be exhibited between the features and targets. Based on the synthetic data set, the processing conditions that output SET voltages with minimal dispersion between devices would consist of a temperature between 90 to 110 degrees Celsius, baking time greater than 6 hours, using a copper bottom electrode, and honey with carbon nanotubes as the insulator film.

V. MACHINE LEARNING BASED MODELING AND PREDICTION

A. Methodology

The 2-phase synthetic data assisted prediction approach presented in Section IV provides an effective method to predict the statistical metrics of bio-RRAM performance without requiring a large training dataset. However, since the prediction targets for this approach are statistical metrics, e.g., mean, minimum, maximum, etc., they only provide coarse grained information about the RRAM sample's performance. In many scenarios, more fine-grained information is needed in order to facilitate the decision making process during the fabrication. To this end, we have designed and developed a new approach for fine-grained modeling and prediction, without increasing the size of the training dataset.

The key idea of this approach is to repurpose the learning task: instead of predicting the actual performance metric or statistical metric for the RRAM devices, we develop a model which captures the detailed distribution of the performance measurements, i.e., SET voltages in this case. The ultimate goal is to enable a comprehensive representation and prediction for the devices performance. To do this, we train machine learning models to predict the likelihood that a given set voltage value for will be produced by a specified device sample.

Figure 5 shows the proposed approach, which also involves two phases. In Phase I, the Kernel Density estimator [33] is constructed and is used to process the experimental dataset containing the eight bio-RRAM samples. Specifically, the data for each sample device is fed to the Kernel Density estimator, including all values of the set voltage pertaining to that sample. Then for each device sample, every instance of SET voltage is taken as input in its respective fitted KDE model. This calculated the probability of observing that value in that sample. The probability values are then added to the data set to be used as the target. Phase I represents the process of learning task conversion. In Phase II, the dataset produced by Phase I is

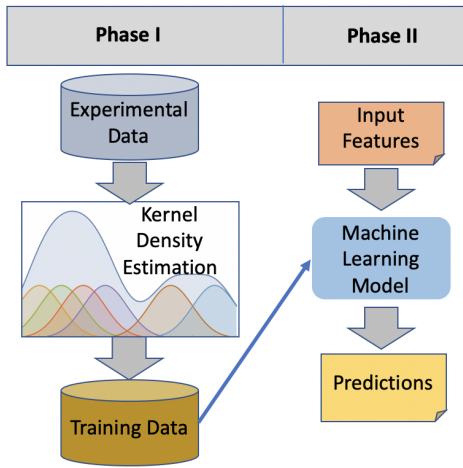


Fig. 5. Machine Learning Based Probability Modeling and Prediction

used to train a machine learning model to learn the correlation between microfabrication process conditions and the device’s performance metric distribution, in the form of the likelihood for any given performance value. For testing, we run extensive tests to use the trained model to produce a comprehensive distribution of SET voltage values, given a number of generated input features, including process conditions, hypothetical SET voltage values. Note that during the whole process, only experimental data is used, and no synthetic data is needed. This will eliminate the potential bias brought in by synthetic data.

B. Experimental Design

The objective of this approach is to determine if its possible to predict the complete set of performance metrics of the RRAM device given new processing conditions. This would speed up development of the device and minimize the cost of failed attempts during the fabrication process.

The test consisted of constructing a data set with new potential processing conditions, in a similar fashion as the synthetic data in the approach described in Section IV. New combinations of RRAM manufacturing conditions were composed using the feature materials including bottom electrode material, top electrode material, resistive switching film, baking temperature, baking time, and SET voltage. Temperature values were progressively incremented by 10 degrees, starting at 90 degrees Celsius up to 140 degree Celsius. Baking time duration values to 10 hours incremented by half hours steps. There were 176 individual simulated processing conditions created in the test set. The set voltage was represented by values ranging from 0 to 10, at 0.25 increments. These values were added as the set voltage column in the data set, giving each sample a total of 41 instances. For the machine learning model, we choose AdaBoost and Random Forest.

C. Evaluation

To evaluate the effectiveness of the 2-phase machine learning approach presented in Section V-A, an extensive set of

experiments have been carried out. In each experiment, we leave one sample out for testing. This specific testing sample is not included in the training process. Once the model is trained using the rest 7 samples, the testing sample is used to evaluate the prediction. Specifically, The testing data is constructed by replicating the process conditions for the specified sample and adding a SET voltage feature. The SET voltage values were simulated by creating a range of numbers from 0 to 10 at increments of 0.25. The dataset was composed of rows pertaining to only one test sample. The test sample was then taken as input by the trained Random Forest Regression and AdaBoost models, to have the probability predicted over each SET voltage value. The results were then compared to a true distribution data set which were obtained from the fitted KDE model for real experimental measurements from the testing sample.

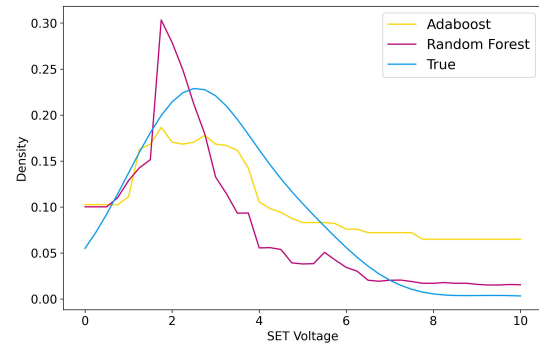


Fig. 6. Performance Prediction for Sample 1

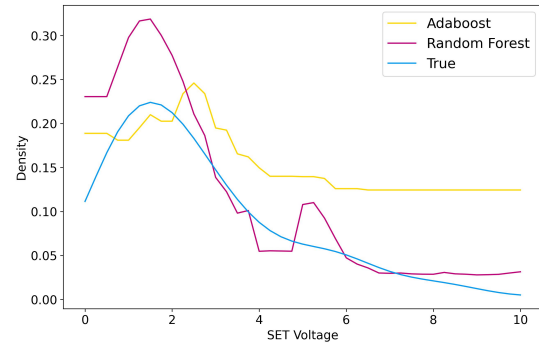


Fig. 7. Performance Prediction for Sample 5

Figure 6 and Figure 7 show two examples of the prediction results, for Sample 2 and 5, respectively. The figures plot the true distribution of the corresponding sample (blue line), and the predicted distributions from the AdaBoost (yellow line) and Random Forest (purple line). As shown in the figures, our approach is able to accurately capture the main trend in the performance distribution, indicating great potentials

for enabling more cost-effective microfabrication for RRAM devices.

To further evaluate and quantify the similarities of the predicted distributions and the true distribution, their Hausdorff distance is calculated. The Hausdorff distance is a measure of dissimilarity between two sets of points. For any two sets of points, set A and B, the Hausdorff distance is the maximum distance for any point in A to its nearest neighbor in B [34]. Table VI shows the comparison of the predicted distribution line from the true data.

TABLE VI
HAUSDORFF DISTANCE OF EACH SAMPLE TO THE TRUE DISTRIBUTION AS PREDICTED BY THE REGRESSION MODELS.

Sample ID	AdaBoost	Random Forest
1	0.0786	0.0734
2	0.0775	0.0458
3	0.2706	0.0441
4	0.1027	0.0167
5	0.1081	0.0968
6	0.4176	0.3632
7	0.1869	0.1923
8	0.2577	0.2669

The Hausdorff distance for all samples are below 0.5, indicating the predicted distribution curves are generally accurate, or similar to their original curve. Note that in these results, the sample used in testing is not included during Phase I or in the training process of Phase II. Therefore, all testing samples are unseen data for the machine learning models. It is worth noting that the Hausdorff distance for Sample 6 is slightly higher than others. This is attributed to the resistive switching film feature in this sample. There is unbalance of values for the samples in the dataset, as most of the samples used pure honey (label 0) as the resistive switching film. We anticipate that as more data is acquired, the prediction accuracy will be improved. Considering there are only eight sample used in this approach, and there is no synthetic data being generated during the process, achieving the level of accuracy is a significant contribution to RRAM microfabrication, demonstrating great potentials for supporting more advanced fabrication processes.

VI. CONCLUSION

With the increasing demand for more powerful computing systems, tremendous energy consumption and electronic wastes become significant side effects which must be dealt with. A potential solution to simultaneously address these two issues is by “brain-like” and “green” neuromorphic computing with energy-efficient operation and biodegradable disposals. However, due to the complexity of the microfabrication process, developing those hardware is extremely difficult, and the current practice is based on trial-and-error, which is neither efficient nor scalable. In this paper, we present our research in utilizing machine learning techniques to aid bio-RRAM design and development. Specifically, we have developed two distinct methodologies to address the fundamental challenge in this field: lack of large scale training data.

The first approach leverages sequential machine learning data synthesis to produce synthetic data for training, without adding more costly processes to produce real samples. The second approach is based on a learning task conversion, which models the problem in the space of probability, and generates a comprehensive, fine-grained distribution of the performance metrics for any new bio-RRAM devices. These approaches bridge the gaps in the state-of-the-art, and pave the way to more efficient and effective design of the next-generation RRAM devices for green neuromorphic computing.

Work is ongoing in several directions. First, we will explore other performance metrics of bio-RRAM, such as non-ideal effects caused by the fabrication process, and leverage the machine learning based approaches to detect those effects. This is essential for supporting neural network on the devices. Second, we will investigate the learning capabilities of bio-RRAM devices using typical deep learning benchmarks. Finally, building on top of these findings, we will design and develop tools to facilitate and evaluate hardware/software co-design for neuromorphic computing.

ACKNOWLEDGMENT

This research is supported in part by the National Science Foundation, ECCS-2104976.

REFERENCES

- [1] J. Backus, “Can Programming Be Liberated from the Von Neumann Style?: A Functional Style and Its Algebra of Programs,” *Commun. ACM*, vol. 21, no. 8, pp. 613–641, 1978.
- [2] A. Sandberg and N. Boström, “Whole Brain Emulation: A Roadmap,” Future of Humanity Institute, Oxford University, Tech. Rep. 2008-3, 2008.
- [3] D. Monroe, “Neuromorphic computing gets ready for the (really) big time,” *Commun. ACM*, vol. 57, no. 6, p. 13–15, Jun. 2014.
- [4] D. Marković, A. Mizrahi, D. Querlioz, and J. Grollier, “Physics for neuromorphic computing,” *Nature Reviews Physics*, vol. 2, no. 9, pp. 499–510, 2020.
- [5] A. Khiat, S. Cortese, A. Serb, and T. Prodromakis, “Resistive Switching of Pt/TiOx /Pt Devices Fabricated on Flexible Parylene-C Substrates,” *Nanotechnology*, vol. 28, p. 025303, 02 2017.
- [6] J. Kim, A. I. Inamdar, Y. Jo, H. Woo, S. Cho, S. M. Pawar, H. Kim, and a. Im, “Effect of Electronegativity on Bipolar Resistive Switching in a WO3-Based Asymmetric Capacitor Structure,” *Applied Materials and Interfaces*, vol. 8, pp. 9499 – 9505, 14 2016.
- [7] L. Zhang, L. Zhu, X. Li, Z. Xu, W. Wang, and X. Bai, “Resistive Switching Mechanism in the One Diode-One Resistor Memory Based on p+-Si/n-ZnO Heterostructure Revealed by In-situ TEM,” *Scientific Reports*, vol. 7, p. 45143, 2017.
- [8] S. Chandrasekaran, F. M. Simanjuntak, R. Saminathan, D. Panda, and T.-Y. Tseng, “Improving Linearity by Introducing Al in HfO2 as a Memristor Synapse Device,” *Nanotechnology*, vol. 30, p. 445205, 44 2019.
- [9] G. Zhou, L. Xiao, S. Zhang, B. Wu, X. Liu, and A. Zhou, “Mechanism for an Enhanced Resistive Switching Effect of Bilayer NiOx/TiO2 for Resistive Random Access Memory,” *Journal of Alloys and Compounds*, vol. 722, pp. 753 – 759, 10 2017.
- [10] A. Melianas, T. J. Quilll, G. LeCroy, Y. Tuchman, H. v. Loo, S. T. Keene, A. Giovannitti, H. R. Lee, I. McCulloch, and A. Salleo, “Temperature-resilient solid-state organic artificial synapses for neuromorphic computing,” *Science Advances*, vol. 6, no. 7, p. eabb2958, 2020.
- [11] H. J. Kim, H. Zheng, J.-S. Park, D. H. Kim, C. J. Kang, J. T. Jang, D. H. Kim, and T.-S. Yoon, “Artificial Synaptic Characteristics with Strong Analog Memristive Switching in a Pt/CeO2/Pt structure,” *Nanotechnology*, vol. 28, no. 28, p. 285203, 2017.

- [12] R. Waser, R. Dittmann, G. Staikov, and K. Szot, "Redox-Based Resistive Switching Memories - Nanoionic Mechanisms, Prospects, and Challenges," *Advanced Materials*, vol. 21, no. 25-26, pp. 2632–2663, 2009.
- [13] J. J. Yang, D. B. Strukov, and D. R. Stewart, "Memristive Devices for Computing," *Nature Nanotechnology*, vol. 8, pp. 13–24, 12 2012.
- [14] H. S. P. Wong and S. Salahuddin, "Memory Leads the Way to Better Computing," *Nature Nanotechnology*, vol. 10, pp. 191–194, 2015.
- [15] Y. H. Jung, T.-H. Chang, H. Zhang, C. Yao, Q. Zheng, V. W. Yang, H. Mi, M. Kim, S. J. Cho, D.-W. Park *et al.*, "High-performance green flexible electronics based on biodegradable cellulose nanofibril paper," *Nature communications*, vol. 6, no. 1, pp. 1–11, 2015.
- [16] J.-W. Chang, C.-G. Wang, C.-Y. Huang, T.-D. Tsai, T.-F. Guo, and T.-C. Wen, "Chicken albumen dielectrics in organic field-effect transistors," *Advanced materials*, vol. 23, no. 35, pp. 4077–4081, 2011.
- [17] J. A. Hagen, W. Li, A. Steckl, and J. Grote, "Enhanced emission efficiency in organic light-emitting diodes using deoxyribonucleic acid complex as an electron blocking layer," *Applied Physics Letters*, vol. 88, no. 17, p. 171109, 2006.
- [18] V. Gupta, S. Kapur, S. Saurabh, and A. Grover, "Resistive random access memory: a review of device challenges," *IETE Technical Review*, vol. 37, no. 4, pp. 377–390, 2020.
- [19] Y.-C. Chang, H.-J. Liu, K.-W. Lin, W.-Y. Huang, and Y.-L. Hsu, "A biodegradable gelatin substrate and its application for crack suppression of flexible gelatin resistive memory device," *Advanced Electronic Materials*, p. 2101014, 2022.
- [20] Y.-C. Chen, H.-C. Yu, C.-Y. Huang, W.-L. Chung, S.-L. Wu, and Y.-K. Su, "Nonvolatile bio-memristor fabricated with egg albumen film," *Scientific reports*, vol. 5, no. 1, pp. 1–12, 2015.
- [21] P. T. Chandane, T. D. Dongale, P. B. Patil, and A. P. Tiwari, "Organic resistive switching device based on cellulose-gelatine microcomposite fibers," *Journal of Materials Science: Materials in Electronics*, vol. 30, no. 24, pp. 21 288–21 296, 2019.
- [22] Z. W. Dlamini, S. Vallabhapurapu, S. Wu, T. S. Mahule, A. Srivivasan, and V. S. Vallabhapurapu, "Resistive switching memory based on chitosan/polyvinylpyrrolidone blend as active layers," *Solid State Communications*, vol. 345, p. 114677, 2022.
- [23] Z. Lim, I. Tayeb, Z. Hamid, M. Ain, A. Hashim, J. Abdullah, F. Zhao, and K. Cheong, "Switching dynamics and conductance quantization of *aloe* polysaccharides-based device," *IEEE Transactions on Electron Devices*, vol. 66, no. 7, pp. 3110–3117, 2019.
- [24] Y. Xing, B. Sueoka, K. Y. Cheong, and F. Zhao, "Nonvolatile resistive switching memory based on monosaccharide fructose film," *Applied Physics Letters*, vol. 119, no. 16, p. 163302, 2021.
- [25] S. P. Park, Y. J. Tak, H. J. Kim, J. H. Lee, H. Yoo, and H. J. Kim, "Analysis of the bipolar resistive switching behavior of a biocompatible glucose film for resistive random access memory," *Advanced Materials*, vol. 30, no. 26, p. 1800722, 2018.
- [26] B. Sueoka, K. Y. Cheong, and F. Zhao, "Natural biomaterial honey-based resistive switching device for artificial synapse in neuromorphic systems," *Applied Physics Letters*, vol. 120, no. 8, p. 083301, 2022.
- [27] X. Li, H. Wang, B. Wang, and Y. Guan, "Machine learning methods for prediction analyses of 4H-SiC microfabrication via femtosecond laser processing," *Journal of Materials Research and Technology*, vol. 18, pp. 2152–2165, 2022.
- [28] F. Zhang and T. Zhou, "Process parameter optimization for laser-magnetic welding based on a sample-sorted support vector regression," *Journal of Intelligent Manufacturing*, vol. 30, no. 5, pp. 2217–2230, 2019.
- [29] J. Maudes, A. Bustillo, A. J. Guerra, and J. Ciurana, "Random forest ensemble prediction of stent dimensions in microfabrication processes," *The International Journal of Advanced Manufacturing Technology*, vol. 91, no. 1, pp. 879–893, 2017.
- [30] A. A. Sivkov, Y. Xing, K. Y. Cheong, X. Zeng, and F. Zhao, "Investigation of Honey Thin Film as a Resistive Switching Material for Nonvolatile Memories," *Materials Letters*, vol. 271, p. 127796, 2020.
- [31] K. El Emam, *Practical synthetic data generation : balancing privacy and the broad availability of data / Khaled El Emam, Lucy Mosquera, and Richard Hoptroff.*, 1st ed. Sebastopol, CA: O'Reilly Media, 2020.
- [32] E. A. Lopez-Rojas and S. Axelsson, "Money laundering detection using synthetic data," in *Annual workshop of the Swedish Artificial Intelligence Society (SAIS)*. Linköping University Electronic Press, Linköping universitet, 2012.
- [33] S. Węglarczyk, "Kernel density estimation and its application," *ITM Web of Conferences*, vol. 23, p. 00037, 01 2018.
- [34] A. A. Taha and A. Hanbury, "An Efficient Algorithm for Calculating the Exact Hausdorff Distance," *IEEE Transactions on Pattern Analysis and Machine Intelligence*, pp. 1–1, 03 2015.